# Heme Nitrosylation of Deoxyhemoglobin by S-Nitrosoglutathione Requires Copper*

### Andrea A. Romeo, John A. Capobianco, and Ann M. English‡

*From the Department of Chemistry and Biochemistry, Concordia University, 1455 de Maisonneuve Boulevard West, Montreal, Quebec H3G 1M8, Canada*

NO reactions with hemoglobin (Hb) likely play a role in blood pressure regulation. For example, NO exchange between Hb and S-nitrosoglutathione (GSNO) has been reported *in vitro*. Here we examine the reaction between GSNO and deoxyHb (HbFe$^{II}$) in the presence of both Cu(I) (2,9-dimethyl-1, 10-phenanthroline (neocuproine)) and Cu(II) (diethylenetriamine-$N,N,N',N'',N''$-pentaacetic acid) chelators using a copper-depleted Hb solution. Spectroscopic analysis of deoxyHb (HbFe$^{II}$)/GSNO incubates shows prompt formation (<5 min) of ~100% heme-nitrosylated Hb (HbFe$^{II}$NO) in the absence of chelators, 46% in the presence of diethylenetriamine-$N,N,N',N'',N''$-pentaacetic acid, and 25% in the presence of neocuproine. Negligible (<2%) HbFe$^{II}$NO was detected when neocuproine was added to copper-depleted HbFe$^{II}$/GSNO incubates. Thus, HbFe$^{II}$NO formation *via* a mechanism involving *free* NO generated by Cu(I) catalysis of GSNO breakdown is proposed. GSH is a source of reducing equivalents because extensive GSSG was detected in HbFe$^{II}$/GSNO incubates in the absence of metal chelators. No S-nitrosation of HbFe$^{II}$ was detected under any conditions. In contrast, the NO released from GSNO is directed to Cys$\beta^{93}$ of oxyHb in the absence of chelators, but only metHb formation is observed in the presence of chelators. Our findings reveal that the reactions of GSNO and Hb are controlled by copper and that metal chelators do not fully inhibit NO release from GSNO in Hb-containing solutions.

Possible exchange of NO between thiols and hemoglobin (Hb)[1] in red blood cells (RBCs) has been the focus of intense interest recently (1, 2). It has been suggested that GSNO or S-nitroso-L-cysteinyl could act as an NO$^+$ donor to Cys$\beta^{93}$ of oxyhemoglobin (HbFe$^{II}$O$_2$) in a *trans*-S-nitrosation reaction (3). However, we have shown that free NO must first be released from GSNO (4), the S-nitroso form of the dominant thiol in the RBC (5), or S-nitroso-L-cysteinyl[2] in a Cu(I)-catalyzed reaction. S-Nitrosation of Cys$\beta^{93}$ then occurs in a Cu(II)-catalyzed reaction (4) as reported also for Cys$^{34}$ of bovine serum albumin (6). For Hb to function as a blood pressure regulator in an O$_2$-sensitive manner, release of NO from Cys$\beta^{93}$ of HbFe$^{II}$ is necessary (7). One possibility is that NO is delivered to tissues *via* S-nitrosation from Cys$\beta^{93}$ to GSH or another thiol (8) that promotes NO transport across the RBC.

$$HbSNO + RSH \rightleftharpoons HbSH + RSNO$$
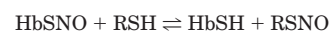
REACTION 1

Recently it has been suggested that delivery to tissues of all of the NO bound to Cys$\beta^{93}$ of Hb would result in extensive vasodilation, which would be fatal (9). Hence, it was proposed that most of the NO released from Cys$\beta^{93}$ is actually captured by HbFe$^{II}$. Capture of NO released from GSNO is also possible and would compete with the exit of NO from the RBC. In fact, Spencer *et al.* (10) reported direct reductive cleavage of GSNO by HbFe$^{II}$ and capture of the released NO by another Fe$^{II}$ center (Hb'Fe$^{II}$).

$$HbFe^{II} + GSNO + H^+ \rightleftharpoons HbFe^{III} + GSH + NO$$

$$Hb'Fe^{II} + NO \rightleftharpoons Hb'Fe^{II}NO$$
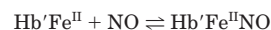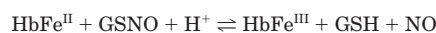
REACTIONS 2 AND 3

A trace amount of Cu(I) serves as a highly efficient catalyst of S-nitrosothiol breakdown (11). We have suggested that neocuproine, a Cu(I)-specific chelator, inhibits NO release from GSNO in solutions of HbFe$^{II}$O$_2$ (4). Therefore, we considered it likely that neocuproine would also inhibit NO release from GSNO in solutions containing HbFe$^{II}$. To distinguish between direct reductive cleavage of GSNO by HbFe$^{II}$ (Reaction 2) and Cu(I)-catalyzed release (Reaction 4), it is necessary to remove all trace copper or prevent its turnover *via* redox cycling using GSH (Reaction 5) or another donor in the Hb-containing solutions.

$$Cu(I) + GSNO + H^+ \rightleftharpoons Cu(II) + GSH + NO$$

$$Cu(II) + GSH \rightleftharpoons Cu(I) + ½ GSSG + H^+$$
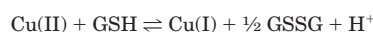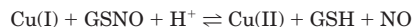
REACTIONS 4 AND 5

Here we report the results of a detailed examination of HbFe$^{II}$/GSNO incubates after 5 min in the presence of preferential chelators of Cu(I) (neocuproine) and Cu(II) (DTPA). Solutions of HbFe$^{II}$ that were not dialyzed and solutions that underwent exhaustive dialysis *versus* EDTA were used. Our direct spectroscopic and ESI-MS analyses reveal that NO re-

---

‡ To whom correspondence should be addressed. Tel.: 514-848-3338; Fax: 514-848-2868, E-mail: english@vax2.concordia.ca.

[1] The abbreviations used are: Hb, hemoglobin; DTPA, diethylenetriamine-$N,N,N',N'',N''$-pentaacetic acid; ESI, electrospray ionization; MS, mass spectrometry; FTIR, Fourier transform infrared; GSNO, glycine $N$-($N$-L-γ-glutamyl-S-nitroso-L-cysteinyl); HbFe$^{III}$, metHb; HbFe$^{II}$, deoxyHb; HbFe$^{II}$NO, heme-nitrosylated Hb; HbFe$^{III}$NO, metnitrosylHb; HbFe$^{II}$O$_2$, oxyHb; HbSNO, Hb S-nitrosated at Cys$\beta^{93}$; ICP, inductively coupled plasma; NaPi, sodium phosphate buffer; neocuproine, 2,9-dimethyl-1,10-phenanthroline; RBC, red blood cell.

[2] A. A. Romeo, J. A. Capobianco, and A. M. English, unpublished observations.

lease from GSNO is <2% in the presence of neocuproine in HbFe$^{II}$/GSNO solutions containing dialyzed Hb. HbFe$^{II}$NO formation, and hence GSNO breakdown, is ~100% within 5 min in the absence of chelators. HbFe$^{II}$NO formation is decreased by ~50–75% in the presence of DTPA and neocuproine and in solutions containing dialyzed Hb without neocuproine. Because trace copper was found in all reagents by ICP-MS, these observations are consistent with Cu(I)-catalyzed release of NO (Reaction 4).

The source of the reducing equivalents for the prompt Cu(I)-catalyzed reductive cleavage of GSNO is also of interest. Extensive GSSG was formed in HbFe$^{II}$/GSNO incubates in the absence of metal chelators, indicating that GSH is the main source of reducing equivalents under these conditions (Reaction 5). We detected less GSSG than expected by ESI-MS in HbFe$^{II}$/GSNO incubates containing DTPA, although we observed ~50% GSNO breakdown. This suggested HbFe$^{II}$ as a possible additional source of reducing equivalents to [Cu(II)-(DTPA)]$^{2-}$ because related EDTA complexes were shown to be redox-active with Hb (12). Careful examination of the absorption (optical and FTIR) spectra revealed the presence of HbFe$^{III}$. Thus, our results indicate that the direct reduction of GSNO by HbFe$^{II}$ is unlikely to play a role in NO transport in RBCs. Nonetheless, HbFe$^{II}$ may indirectly provide a source of electrons for the reductive cleavage of GSNO or other *S*-nitrosothiols *in vivo*.

The realization that commonly used Cu(I) (neocuproine) and Cu(II) chelators (EDTA and DTPA) may not always prevent copper turnover is an important consideration in deciphering mechanisms of *S*-nitrosothiol signaling and NO biochemistry in general. Although neocuproine, a tight binding Cu(I) chelator ($K_d = 1.2 \times 10^{-19}$ M$^2$) (13, 14), is a better inhibitor than DTPA of GSNO breakdown (Reaction 4) in Hb-containing solutions, dialysis of the Hb samples and neocuproine addition were necessary to obtain negligible GSNO breakdown.

Finally, the prompt changes in HbFe$^{II}$O$_2$ on incubation with GSNO are compared with those observed for the HbFe$^{II}$ incubates. The key results of this comparison are that in the absence of chelators, *S*-nitrosation of Cys$\beta^{93}$ of the oxy protein is extensive, and this competes with NO capture by the Fe$^{II}$O$_2$ heme to form HbFe$^{III}$ and NO$_3^-$. In contrast, no *S*-nitrosation of the deoxy protein is detected, suggesting that all of the NO released from GSNO is captured by the Fe$^{II}$ heme.

<div align="center">EXPERIMENTAL PROCEDURES</div>
<div align="center">*Materials*</div>

Human hemoglobin A was obtained from Sigma and used without further purification. Nanopure water (specific resistance, 18 MΩ-cm) obtained from a Millipore Simplicity water purification system and treated with Chelex-100 (Sigma) to remove trace metal ions was used to prepare all H$_2$O solutions. The reactions were carried out in 200 mM sodium phosphate buffer, pH 7.2 (NaPi), prepared from sodium phosphate salts (Fisher) in nanopure H$_2$O. Stock solutions of 15 mM diethylenetriamine-*N,N,N′,N″,N″*-pentaacetic acid (DTPA; ICN) and 650 µM 2,9-dimethyl-1,10-phenanthroline (neocuproine; Sigma) were prepared in NaPi. Stock solutions of 250 mM GSNO (Cayman) in NaPi were prepared just before use in a glove bag (Aldrich) under nitrogen, and the GSNO concentrations were determined spectrophotometrically ($\epsilon_{333.5\ nm} = 774$ M$^{-1}$ cm$^{-1}$) (15). GSH and GSSG were obtained from Sigma, and N$_2$ and NO gases were from Praxair. NO was purged into a 10% KOH water solution before use (16).

<div align="center">*Methods*</div>

*Preparation and Optical Spectroscopy of Hb Samples*—Typically 1 g of lyophilized metHb (HbFe$^{III}$) from the bottle was dissolved in 2 ml of NaPi. After 2 min of centrifugation at 12,000 rpm, the precipitate was discarded, and the dark red solution of HbFe$^{III}$ was stored at 4 °C prior to use. An aliquot (10 µl) of the Hb solution was pipetted onto a 13-mm CaF$_2$ window of a dismountable FTIR type cell (Harrick). The cell was immediately assembled using a 6-µm Teflon spacer (Harrick) and

placed in a custom-made bracket in a Beckman DU 650 UV-visible spectrophotometer. HbFe$^{III}$ concentrations were found to be 32 mM in heme assuming $\epsilon_{500\ nm} = 10$ mM$^{-1}$ cm$^{-1}$/heme and $\epsilon_{630\ nm} = 4.4$ mM$^{-1}$ cm$^{-1}$/heme (17, 18). This was confirmed by diluting the samples 10$^3$-fold, adding potassium ferricyanide and excess KCN (BDH chemicals), and reading the absorbance of the CN$^-$ adduct at 540 nm ($\epsilon_{540\ nm} = 11.0$ mM$^{-1}$ cm$^{-1}$/heme) in a 1-cm cuvette on a Beckman spectrophotometer.

HbFe$^{II}$ was prepared in the glove bag under N$_2$ by treating HbFe$^{III}$ with equimolar sodium dithionite (Fisher) (19) followed by desalting on a 1.6 × 2.5-cm HiTrap Sephadex G-25 column (Amersham Biosciences), and the HbFe$^{II}$ concentration was calculated using $\epsilon_{555\ nm} = 12.5$ mM$^{-1}$ cm$^{-1}$/heme (20). HbFe$^{II}$O$_2$ was prepared from HbFe$^{II}$ by introducing a small volume of air into the sample using a syringe; for example, 720 µl of air was added to 200 µl of a 32 mM heme sample. A single addition of O$_2$ in slight excess (8.5 µmol of O$_2$/8 µmol of heme) yielded fully oxygenated Hb as indicated by the Soret spectrum recorded following a 5-min equilibration. HbFe$^{II}$NO and HbFe$^{III}$NO were prepared from HbFe$^{II}$ and HbFe$^{III}$ on exposure to NO gas. The optical spectra were recorded using a scan time of 1200 nm/min. Use of the FTIR type cell to record the optical spectra of the products formed in the HbFe$^{II}$/GSNO incubates allowed measurements to be made at close to physiological concentrations of Hb (2–4 mM) (21).

*Preparation of Dialyzed Hb Samples*—Approximately 500 mg of HbFe$^{III}$ was dissolved in 5 ml of 100 mM Na$_2$EDTA (Sigma), pH 7.0, and allowed to stand for 30 min. This solution was dialyzed at 4 °C *versus* 500 ml of 10 mM Na$_2$EDTA, pH 7.0, which was replaced with fresh solution six times in 24 h. The dialysis was continued *versus* EDTA-free H$_2$O, which was replaced with fresh solution 12 times in 48 h. After dialysis, HbFe$^{III}$ was lyophilized and dissolved in NaPi to a concentration of 30 mM heme.

*ICP-MS Analysis*—A PE Sciex Elan 6000 ICP-MS with a cross-flow nebulizer and a Scott type spray chamber was used to determine the amount of copper in the Hb and GSNO samples and in the buffers (see Table I). The RF power was 1000 W, and the argon flow was 0.85 liter/min, which gave the best sensitivity as determined by the recommended optimization procedure. The optimum lens voltage was determined by maximizing rhodium sensitivity, and the data were acquired in the pulse count mode (22). Stock Hb solutions in NaPi were added to 50 µl of 30% H$_2$O$_2$ (ACP Chemicals, Inc.) and 500 µl of concentrated HNO$_3$ (Omni*Trace* Ultra high purity, EM Science) to give a final heme (iron) concentration of 4.3 mM, and the samples were ashed using a Bunsen burner. The residue was dissolved in 10 ml of 5% (v/v) HNO$_3$, and ICP-MS analyses for copper and iron were performed. An internal standard of 9 nM (0.500 ppb) manganese prepared from a 1000 ppm manganese standard solution (ACP Chemicals, Inc.) was added to all of the solutions. The standard curves were prepared by diluting 1000 ppm copper and iron standard solutions (ACP Chemicals, Inc.) in 5% (v/v) HNO$_3$ and nanopure water to give 0–8 µM (0–0.500 ppm) copper and 0–9 µM (0–0.500 ppm) iron. All of the reported ICP-MS data are the results of at least triplicate experiments, and in all cases the standard deviations were <5%.

*FTIR Analysis*—Approximately 20 µl of Hb (28 mM heme) in NaPi was added by syringe onto a 13-mm CaF$_2$ window in the glove bag under N$_2$ where necessary. The FTIR cell was immediately assembled with a 250-µm Teflon spacer (Harrick), and the spectra were recorded at 25 °C on a Nicolet Magna-IR 550 spectrometer with a MCT detector cooled to 77 K and purged with dry air from a Whatman FTIR Purge (model 75-52). All of the reported spectra are averages of 500 scans recorded in 5.52 min at a resolution of 2 cm$^{-1}$ using a Happ-Genzel apodization with a velocity and aperture of 4.4303 cm/s and 2, respectively. Omnic (Nicolet) software was used for subtraction, base-line correction, smoothing, and Fourier transform self-deconvolution employing a half-width-at-half-height of 0.6 cm$^{-1}$ and an enhancement (K factor) of 1. Subtraction of water vapor absorption from the spectra was performed by the method of Dong *et al.* (23, 24).

*ESI-MS Analysis*—Stock Hb solutions (28 mM heme) in NaPi were diluted 10$^{-3}$-fold with H$_2$O to give ~0.5 µg/µl protein. The aliquots were infused into the ESI source of the mass spectrometer (ThermoFinnigan SSQ 7000) by flow injection from the high performance liquid chromatography (Agilent 1090) using a 100-µl loop (but no column) at 50 µl/min with 75% CH$_3$CN (0.05% trifluoroacetic acid) as a mobile phase. Stock (250 mM) GSH, GSNO, and GSSG solutions in 200 mM NaPi, pH 7.2, were diluted 500-fold with H$_2$O and 10-fold to 50 µM with 75% CH$_3$CN (0.05% trifluoroacetic acid), and their mass spectra were obtained as for the Hb solutions.

*Multi-component Analysis of the Optical Spectra of Incubates*—The absorbance at a given wavelength is the sum of the absorbances ($A$) of all species at that wavelength: $A = A_x + A_y + A_z + \ldots = \epsilon_x b$ [X] + $\epsilon_y b$

TABLE I

*ICP-MS analysis of copper in stock solutions*

| Sample[a] | Copper | |
|---|---|---|
| | *μM* | *ppm* |
| 5 mM Hb[b] | $19 \pm 3$ | $1.207 \pm 0.191$ |
| 5 mM dialyzed Hb[c] | $2.0 \pm 0.7$ | $0.127 \pm 0.045$ |
| 250 mM GSNO | $1.2 \pm 0.8$ | $0.076 \pm 0.050$ |
| 250 mM GSH | $1.0 \pm 0.6$ | $0.063 \pm 0.038$ |
| 250 mM GSSG | $1.1 \pm 0.7$ | $0.070 \pm 0.044$ |
| 15 mM DTPA | $0.7 \pm 0.3$ | $0.044 \pm 0.019$ |
| 650 μM neocuproine | $1.6 \pm 0.5$ | $0.102 \pm 0.032$ |
| 200 mM NaPi buffer | $0.9 \pm 0.7$ | $0.057 \pm 0.044$ |

[a] All stock solutions were prepared in 200 mM sodium phosphate buffer, pH 7.2

[b] Human Hb (Sigma) from the bottle. 5 mM Hb contains 20 mM heme.

[c] Human Hb following dialysis *versus* EDTA (see "Experimental Procedures").

[Y] + $\epsilon_z b$ [Z] + ..., where $\epsilon_x$ is the molar extinction of *X* at the selected wavelength, *b* is the pathlength (6 μm), and [X] is the molar concentration of *X*. Assuming a limited number of oxidation and coordination states for iron of Hb, the spectra recorded for the incubates were mathematically disassembled into those of their components. Absorbances at the Soret maxima of the Hb species were used to generate *n* Beer's law expressions, from which the concentrations ([X], [Y], [Z], etc.) of the *n* species present in the incubates were obtained. Solutions to the *n* equations with *n* unknowns were obtained using a program at www.1728.com/indexalg.htm. For the HbFe$^{II}$/GSNO incubates, absorbances were recorded at the Soret maxima of the expected heme species HbFe$^{III}$, HbFe$^{III}$NO, HbFe$^{II}$NO, and HbFe$^{II}$. The millimolar extinction coefficients ($\epsilon$ in mM$^{-1}$ cm$^{-1}$) and wavelengths (nm; in parentheses) used are the following: 169 (405), 110 (416), 97 (418), 50 (430) for HbFe$^{III}$; 95.5 (405), 129 (416), 130 (418), 95 (430) for HbFe$^{II}$NO; 113 (405), 137 (416), 136 (418), and 64 (430) for HbFe$^{III}$NO and 62 (405), 92 (416), 99 (418), and 133 (430) for HbFe$^{II}$. The corresponding values for the expected iron states in the HbFe$^{II}$O$_2$/GSNO incubates are: 169 (405) and 116 (415) for HbFe$^{III}$ and 102 (405) and 125 (415) for HbFe$^{II}$O$_2$. The spectra of the components and mixtures were graphed using Origin 6.0 software (Microcal).

## RESULTS

*ICP-MS Analysis*—Because the stability of *S*-nitrosothiols is highly dependent on the copper content, all of the solutions were examined by ICP-MS for trace copper. The results are summarized in Table I and reveal that 19 μM copper was found in 5 mM Hb (20 mM heme) solutions. This decreased to 2 μM copper following dialysis *versus* EDTA. NaPi buffer (200 mM) and the 250 mM stock solutions of GSH and its derivatives were found to contain ~1 μM copper (Table I). These values differ from those reported previously using atomic absorption spectroscopy, where ~50 μM copper was found in solutions containing 5 mM Hb, but <1 μM copper was found in 5 mM dialyzed Hb as well as in NaPi (4). Because ICP-MS is more sensitive, more accurate, and did not show matrix effects (as verified using a manganese internal standard) compared with atomic absorption spectroscopy (25), the present copper analyses are considered more reliable.

*Optical Absorption Spectra*—Fig. 1*a* compares the spectra of HbFe$^{II}$ and HbFe$^{III}$ and their NO adducts in the Soret and visible regions. As expected, high spin Fe$^{II}$ and Fe$^{III}$ hemes exhibit Soret maxima at 430 and 405 nm, respectively, and visible bands at 556 nm (Fe$^{II}$) and 500, 540, and 580 nm (Fe$^{III}$). Soret maxima are observed at 418 nm ($\epsilon$ = 130 mM$^{-1}$ cm$^{-1}$; Fe$^{II}$NO) and 416 nm ($\epsilon$ = 137 mM$^{-1}$ cm$^{-1}$; Fe$^{III}$NO) for the heme-NO adducts of Hb. The corresponding visible bands are at 545 and 575 nm (Fe$^{II}$NO) and 540 and 565 nm (Fe$^{III}$NO). These values agree with those reported previously (19, 26).

The products formed on mixing HbFe$^{II}$ and GSNO under anaerobic conditions were directly probed by comparing their spectra with those in Fig. 1*a*. Evidence for heme-iron nitrosylation is clearly seen in the Soret and visible bands of the
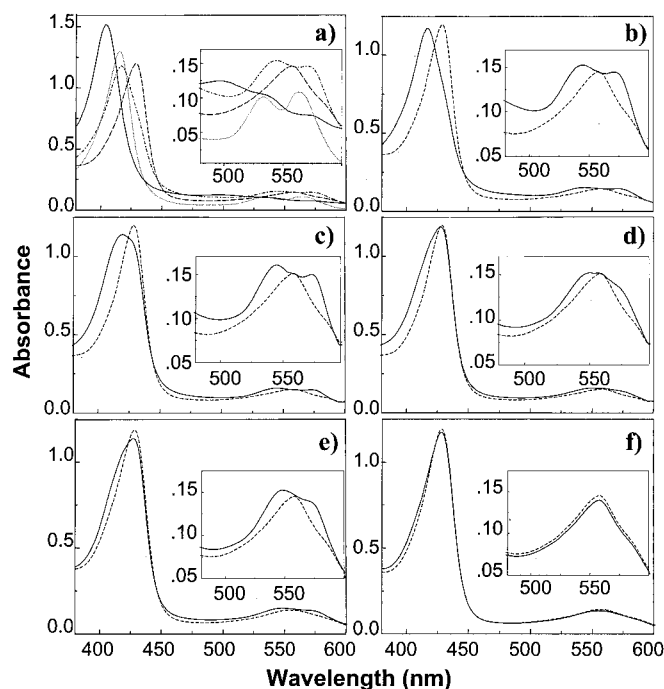


FIG. 1. **Effect of 15 mM GSNO and metal chelators on the visible absorption spectra of 15 mM (heme) HbFe$^{II}$.** *a*, HbFe$^{III}$ (*solid line*), HbFe$^{III}$NO (*dotted line*), HbFe$^{II}$NO (*dotted and dashed line*), and HbFe$^{II}$ (*dashed line*). *b*, HbFe$^{II}$ (*dashed line*) and HbFe$^{II}$ + GSNO after 5 min (*solid line*). *c*, HbFe$^{II}$ (*dashed line*) and HbFe$^{II}$ + GSNO + 200 μM DTPA after 5 min (*solid line*). *d*, HbFe$^{II}$ (*dashed line*) and HbFe$^{II}$ + GSNO + 150 μM neocuproine after 5 min (*solid line*). *e*, dialyzed HbFe$^{II}$ (*dashed line*) and dialyzed HbFe$^{II}$ + GSNO after 5 min (*solid line*). *f*, dialyzed HbFe$^{II}$ (*dashed line*) and dialyzed HbFe$^{II}$ + GSNO + 150 μM neocuproine after 5 min (*solid line*). All of the spectra were recorded in 200 mM sodium phosphate buffer (pH 7.2) at 25 °C in a FTIR cell with a 6-μm Teflon spacer using a scan time of 1200 nm/min.

HbFe$^{II}$/GSNO incubates without chelators (Fig. 1*b*). The Soret maximum blue-shifted from 430 to ~418 nm within 5 min of mixing HbFe$^{II}$ and GSNO, and the visible region resembles that of HbFe$^{II}$NO in Fig. 1*a*. Multi-component analysis of the 5-min spectrum reveals almost complete conversion of HbFe$^{II}$ to HbFe$^{II}$NO (Table II). Thus, rapid release of NO from GSNO occurred in the HbFe$^{II}$/GSNO sample.

Heme nitrosylation is also evident 5 min after mixing HbFe$^{II}$ and GSNO in the presence of 200 μM DTPA (Fig. 1*c*). The extent of nitrosylation is less because the blue shifting of the Soret maximum is less, and the visible maximum of HbFe$^{II}$ at 556 nm is still evident, indicating that DTPA decreases the amount of NO released from GSNO. Multi-component analysis of the spectrum of the 5-min HbFe$^{II}$/GSNO/DTPA incubate reveals the presence of 46% HbFe$^{II}$NO, 44% HbFe$^{II}$, 8.5% HbFe$^{III}$, and 1% HbFe$^{III}$NO (Fig. 2*a* and Table II). When HbFe$^{II}$ and GSNO were mixed in the presence of neocuproine, the spectral changes revealed that significantly less heme nitrosylation occurred (Fig. 1*d*) than in the presence of DTPA, which was confirmed by multi-component analysis (Table II). Approximately 33% heme nitrosylation was found in the incubate of dialyzed HbFe$^{II}$ in the absence of chelators (Fig. 1*e* and Table II), but the addition of 150 μM neocuproine essentially shut down NO release from GSNO (Fig. 1*f*) because 98% HbFe$^{II}$ was found in the 5-min incubate of dialyzed HbFe$^{II}$/GSNO/ neocuproine (Table II).

To compare the heme species formed in HbFe$^{II}$/GSNO incubates with those formed in HbFe$^{II}$O$_2$/GSNO incubates, the spectra of the latter were recorded. The Soret spectra of HbFe$^{II}$O$_2$/GSNO (Fig. 3, *a* and *c*) reveal that HbFe$^{III}$ is formed within 5 min, and multi-component analysis uncovered the

TABLE II

*Hb species present in Hb/GSNO incubates based on analysis of their visible spectra*

15 mM (heme) Hb plus 15 mM GSNO were incubated at room temperature in 200 mM sodium phosphate buffer, pH 7.2. Spectra were recorded 5 min after the start of the incubation. The wavelengths used in the multi-component analysis were the Soret maxima of the expected components, and the extinction coefficients are given under "Methods."

| Incubate | HbFe$^{II}$ | HbFe$^{III}$ | HbFe$^{II}$NO | HbFe$^{III}$NO | HbFe$^{II}$O$_2$ |
|---|---|---|---|---|---|
| | mM | mM | mM | mM | mM |
| HbFe$^{II}$/GSNO | 0.15 | | 14.85 | | |
| HbFe$^{II}$/GSNO/DTPA | 6.59 | 1.28 | 6.97 | 0.16 | |
| HbFe$^{II}$/GSNO/neocuproine | 11.2 | | 3.8 | | |
| HbFe$^{II}$(dial)/GSNO[a] | 10.05 | | 4.95 | | |
| HbFe$^{II}$(dial)/GSNO/neocuproine | 14.72 | | 0.28 | | |
| HbFe$^{II}$O$_2$/GSNO | | 6.85 | | | 8.15 |
| HbFe$^{II}$O$_2$/GSNO/DTPA | | 3.5 | | | 11.5 |
| HbFe$^{II}$O$_2$/GSNO/neocuproine | | 1.8 | | | 13.2 |

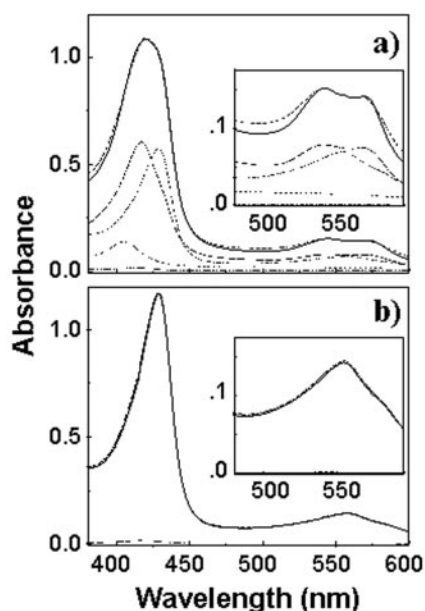[a] HbFe$^{II}$(dial) was dialyzed *versus* EDTA (see "Methods").



FIG. 2. **Multi-component analysis of the visible absorption spectra obtained 5 min after mixing 15 mM (heme) HbFe$^{II}$ and 15 mM GSNO.** *a*, observed spectrum from Fig. 1*c* for HbFe$^{II}$ + GSNO + DTPA (*solid line*); sum (*line with short dashes*) of the spectra of 1.28 mM HbFe$^{III}$ (*dotted line*), 0.16 mM HbFe$^{III}$NO (*line with dashes and two dots*), 6.97 mM HbFe$^{II}$NO (*line with long dashes*), and 6.59 mM HbFe$^{II}$ (*line with dashes and dots*). *b*, observed spectrum from Fig. 1*f* for dialyzed HbFe$^{II}$ + GSNO + 150 μM neocuproine (*solid line*); sum (*line with short dashes*) of the spectra of 0.28 mM HbFe$^{II}$NO (*line with long dashes*) and 14.72 mM HbFe$^{II}$ (*dotted and dashed line*).

presence of ~46% HbFe$^{III}$ and ~54% HbFe$^{II}$O$_2$ (Table II). Significantly less HbFe$^{III}$ formation is detected following mixing of HbFe$^{II}$O$_2$ with GSNO in the presence of DTPA (Fig. 3*b*). This is confirmed by multi-component analysis of the 5-min spectrum, which reveals only 23 and 12% HbFe$^{III}$ formation in HbFe$^{II}$O$_2$/GSNO incubates containing DTPA and neocuproine, respectively. The formation of HbFe$^{III}$ likely occurs from the well characterized reaction of free NO and HbFe$^{II}$O$_2$ (27, 28):

$$HbFe^{II}O_2 + NO \rightleftharpoons HbFe^{III} + NO_3^-$$

REACTION 6

*FTIR Spectra*—FTIR spectroscopy is a valuable probe of protein thiols because the SH stretching vibration $\nu$(SH) falls in a spectral window (~2500 cm$^{-1}$) with minimum H$_2$O and protein absorption (29–31). Although ~5 mM Hb is necessary to observe the weak IR $\nu$(SH) absorption (29–31), comparable Hb concentrations are found in RBCs (~3 mM) (21). The FTIR spectrum of HbFe$^{II}$ in the $\nu$(SH) region recorded in the absence and presence of GSNO and metal chelators (Fig. 4*a*, *spectrum*
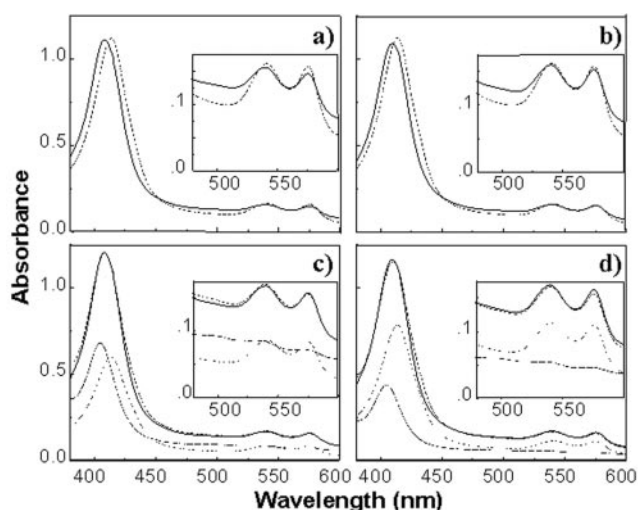


FIG. 3. **Effect of 15 mM GSNO and DTPA on the visible absorption spectra of 15 mM (heme) HbFe$^{II}$O$_2$.** *a*, HbFe$^{II}$O$_2$ (*dashed line*) and HbFe$^{II}$O$_2$ + GSNO after 5 min (*solid line*). *b*, HbFe$^{II}$O$_2$ (*dashed line*) and HbFe$^{II}$O$_2$ + GSNO + 200 μM DTPA after 5 min (*solid line*). *c*, observed spectrum from *a* for HbFe$^{II}$O$_2$ + GSNO after 5 min (*solid line*); sum (*line with short dashes*) of the spectra of 6.85 mM HbFe$^{III}$ (*line with long dashes*) and 8.15 mM HbFe$^{II}$ (*dotted line*). *d*, observed spectrum from *b* for HbFe$^{II}$O$_2$ + GSNO + 200 μM DTPA after 5 min (*solid line*); sum (*line with short dashes*) of the spectra of 3.1 mM HbFe$^{III}$ (*line with long dashes*) and 11.9 mM HbFe$^{III}$ (*dotted line*). See legend for Fig. 1 for experimental details.

*1*) exhibits the three $\nu$(SH) peaks at 2576, 2563, and 2558 cm$^{-1}$ assigned previously to Cys$\beta^{93}$, Cys$\beta^{112}$, and Cys$\alpha^{104}$, respectively (29, 30).

The spectrum of HbFe$^{II}$ plus GSNO (Fig. 4*a*, *spectrum 4*) exhibits a peak for Cys$\beta^{93}$ $\nu$(SH) at 2584 cm$^{-1}$, which is close to that of HbFe$^{II}$NO (2585 cm$^{-1}$). The $\nu$(SH) band for Cys$\beta^{93}$ is also at 2584 cm$^{-1}$ in the HbFe$^{II}$/GSNO/DTPA spectrum (Fig. 4*a*, *spectrum 5*), but in the presence of both DTPA and neocuproine (Fig. 4*a*, *spectrum 2*) Cys$\beta^{93}$ possesses the same $\nu$(SH) (2576 cm$^{-1}$) as HbFe$^{II}$ alone (Fig. 4*a*, *spectrum 1*). These results corroborate those from the analysis of the visible spectra, which revealed that the major Hb species are HbFe$^{II}$NO and HbFe$^{II}$ in the 5-min HbFe$^{II}$/GSNO incubates in the presence of DTPA and neocuproine, respectively. Furthermore, no evidence for HbSNO formation is seen in Fig. 4*a*, because the $\nu$(SH) absorption of Cys$\beta^{93}$ does not appear to lose intensity on exposure to GSNO (Fig. 4*a*, *spectrum 1 versus spectra 2* and *3* and *spectrum 6 versus spectra 4* and *5*).

Loss of Cys$\beta^{93}$ $\nu$(SH) absorption is clearly evident in Fig. 4*b* (*spectrum 1*). Thus, HbSNO formation does occur in the HbFe$^{II}$O$_2$/GSNO incubates in the absence of metal chelators as we reported previously (4). The addition of DTPA prevents loss of Cys$\beta^{93}$ $\nu$(SH) intensity, but the spectrum is not identical to
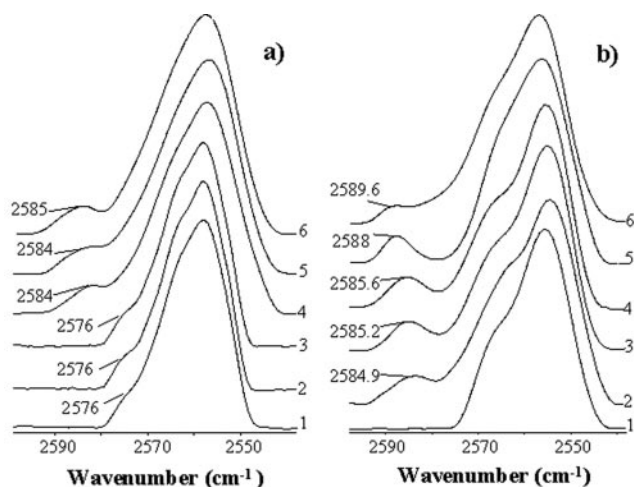
FIG. 4. **Effect of 28 mM GSNO and metal chelators on the FTIR spectra in the ν(SH) region of 28 mM (heme) Hb.** *a*, *spectrum 1*, HbFe$^{II}$; *spectrum 2*, HbFe$^{II}$ + GSNO + 200 μM DTPA + 150 μM neocuproine; *spectrum 3*, HbFe$^{II}$ + GSNO + 150 μM neocuproine; *spectrum 4*, HbFe$^{II}$ + GSNO; *spectrum 5*, HbFe$^{II}$ + GSNO + 200 μM DTPA; *spectrum 6*, HbFe$^{II}$NO. *b*, *spectrum 1*, HbFe$^{II}$O$_2$ + GSNO; *spectrum 2*, HbFe$^{II}$O$_2$ + GSNO + 200 μM DTPA; *spectrum 3*, HbFe$^{II}$O$_2$ + GSNO + 150 μM neocuproine; *spectrum 4*, HbFe$^{II}$O$_2$; *spectrum 5*, HbFe$^{III}$NO; *spectrum 6*, HbFe$^{III}$. All of the spectra were recorded in a 250-μm pathlength FTIR cell 5 min after mixing Hb and GSNO in 200 mM sodium phosphate buffer (pH 7.2) at 25 °C and are the averages of 500 scans at 2-cm$^{-1}$ resolution. Background subtraction, base-line correction, smoothing, and Fourier transform self-deconvolution were performed on the displayed spectra (see text).



FIG. 5. **Deconvolved electrospray mass spectra of the heme-free Hb subunits following incubation with GSNO.** *a*, HbFe$^{II}$ + GSNO. *b*, HbFe$^{II}$O$_2$ + GSNO. Hb and GSNO were incubated in sodium phosphate buffer (pH 7.2) for 5 min at 25 °C and diluted 10$^{-3}$-fold with H$_2$O to give 28 μM heme (~0.5 μg/μl Hb) and 28 μM GSNO. The aliquots (100 μl) were infused into the electrospray source of the mass spectrometer by flow injection at 50 μl/min with 75% CH$_3$CN (0.05% trifluoroacetic acid) as a mobile phase. The capillary temperature was 180 °C, and the spray voltage was 4.0 kV. Under the MS conditions, Hb dissociated into free heme and α- and β-subunits. The unresolved shoulders on the subunit peaks at high mass were caused by sodium adducts.
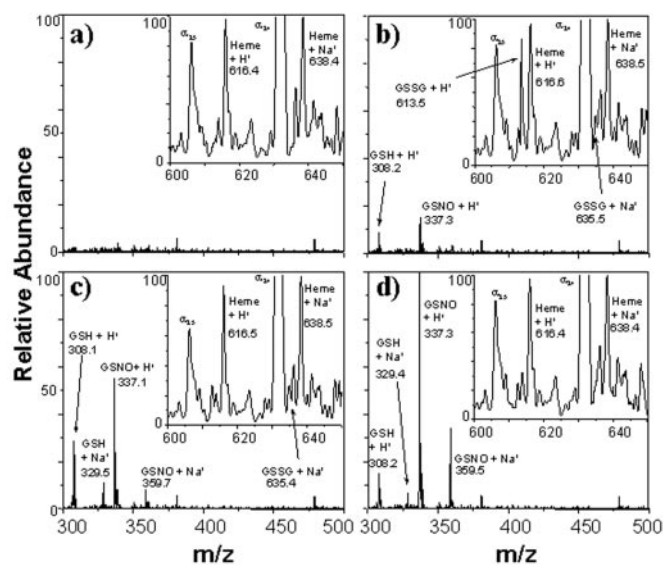


FIG. 6. **Electrospray mass spectra of glutathione products following incubation with HbFe$^{II}$.** *a*, HbFe$^{II}$. *b*, HbFe$^{II}$ + GSNO. *c*, HbFe$^{II}$ + GSNO + 200 μM DTPA. *d*, EDTA-dialyzed HbFe$^{II}$ + GSNO + 150 μM neocuproine. The experimental conditions are the same as those given in the legend to Fig. 5. The peaks labeled α$_{24}$ and α$_{25}$ were caused by α-globin + 24 H$^+$ and α-globin + 25 H$^+$, respectively. All of the peak intensities are relative to the (heme + Na)$^+$ peak at *m/z* 638 (100%).

that of HbFe$^{II}$O$_2$ alone (Fig. 4*b*, *spectrum 2 versus spectrum 4*). Direct monitoring of the heme shows 23% conversion of HbFe$^{II}$O$_2$ to HbFe$^{III}$ within 5 min in the HbFe$^{II}$O$_2$/GSNO/ DTPA incubate (Fig. 3 and Table II). Thus, the FTIR data confirm that DTPA does not prevent release of NO from GSNO (Reaction 4), but it does inhibit *S*-nitrosation of Cysβ$^{93}$ (Fig. 4*b*, *spectrum 2 versus spectrum 1*). The FTIR spectrum of the HbFe$^{II}$O$_2$/GSNO/neocuproine incubate is essentially identical to that of HbFe$^{II}$O$_2$ alone (Fig. 4*b*, *spectrum 3 versus spectrum 4*), which is consistent with the optical results where 88% HbFe$^{II}$O$_2$ was found in the neocuproine incubate (Table II).

*Mass Spectral Analysis*—ESI-MS was used to probe HbSNO formation in the HbFe$^{II}$/GSNO incubates (4). No peak corresponding to *S*-nitrosation of the β-subunit of HbFe$^{II}$ was observed under any conditions with or without metal chelators (Fig. 5*a*) or in the dialyzed HbFe$^{II}$ samples. On the other hand, *S*-nitrosation of the β-subunit was detected following incubation of HbFe$^{II}$O$_2$ with GSNO in the absence of metal chelators (Fig. 5*b*) but not in their presence (data not shown). These MS results support those from FTIR spectroscopy in that HbSNO is formed only in the HbFe$^{II}$O$_2$/GSNO incubates in the absence of metal chelators (Fig. 4*b*, *spectrum 1*).

In the low *m/z* region of the ESI mass spectra, the low molecular weight products formed in the HbFe$^{II}$/GSNO incubates can be monitored. In the absence of metal chelators, a weak GSNO (*m/z* 337) and an intense GSSG peak (*m/z* 613) are observed (Fig. 6*b*) that are not present in the spectrum of Hb alone (Fig. 6*a*). In mass spectrum of the HbFe$^{II}$/GSNO/neocuproine incubate (Fig. 6*d*), GSNO is the dominant glutathione species, and little GSH is present, consistent with decreased GSNO breakdown in the presence of the Cu(I)-specific chelator. In Fig. 6*c*, the GSNO intensity is ~50% of that in the presence of neocuproine, indicating that DTPA is less effective in inhibiting the release of NO from GSNO in Hb solutions. However, a well defined GSSG peak (*m/z* 613) is not observed in Fig. 6*c* as expected if GSH is the major source of electrons for the reduc-
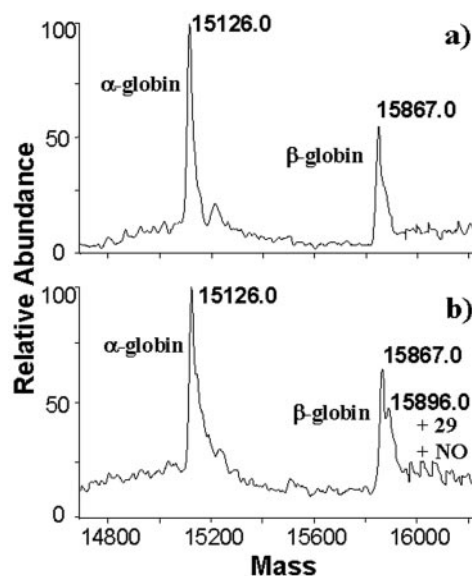
tive cleavage of GSNO (Reactions 4 and 5). A relatively intense GSH peak persists in Fig. 6*c*, and also the optical spectra reveal that HbFe$^{III}$ is formed in the HbFe$^{II}$/GSNO/DTPA incubate (Table II). Because HbFe$^{III}$ is not observed in the HbFe$^{II}$ incubates in the absence of DTPA, [Cu(II)(DTPA)]$^{2-}$ was added to a solution of HbFe$^{II}$ to determine whether this complexed form of copper could oxidize the heme. Multi-component analysis of the absorption spectrum of 4 μM HbFe$^{II}$ and 16 μM [Cu(II)- (DTPA)]$^{2-}$ after 5 min of incubation revealed the presence of

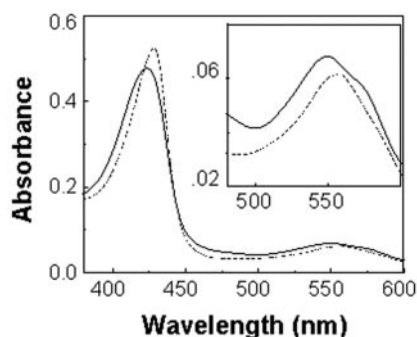FIG. 7. **Visible absorption spectra of 4 $\mu$M (heme) HbFe$^{II}$ with 16 $\mu$M [Cu(II)(DTPA)]$^{2-}$.** *Dashed line*, HbFe$^{II}$; *solid line*, HbFe$^{II}$ + [Cu(II)(DTPA)]$^{2-}$ after 5 min. [Cu(II)(DTPA)]$^{2-}$ was prepared by mixing equimolar solutions of CuSO$_4$ and DTPA. The experimental details are as given in the legend to Fig. 1, except that a 1-cm quartz cuvette was used.

21% HbFe$^{III}$ (Fig. 7). This can be compared with 19% HbFe$^{III}$ formation in the HbFe$^{II}$/GSNO/DTPA incubates (Table II).

### DISCUSSION

Spencer *et al.* (10) have reported that HbFe$^{II}$ can directly reduce GSNO and that the released NO is captured by additional Fe$^{II}$ heme. Because the release of NO from GSNO is known to be Cu(I)-catalyzed (32), we monitored HbFe$^{II}$/GSNO incubates by optical and FTIR spectroscopies to probe changes occurring at the heme and Cys$\beta^{93}$ centers, respectively. In addition, the incubates were analyzed by ESI-MS to examine changes in the mass of the protein and to determine the low molecular weight species produced.

The optical spectra shown in Fig. 1 clearly reveal that trace Cu(I) is required for the release of NO from GSNO (Reaction 4). Essentially no HbFe$^{II}$NO is formed in the HbFe$^{II}$/GSNO incubate containing both copper-depleted Hb (*i.e.* dialyzed Hb in Table I) and neocuproine. The combined data in Tables I and II indicate that total inhibition of Cu(I) catalysis of GSNO breakdown requires removal of most of the copper as well as neocuproine addition to Hb-containing solutions. Thus, the results summarized in Table II are not consistent with direct reduction of GSNO by HbFe$^{II}$ (10) (Reaction 2) when equimolar heme and GSNO are present. Given the rapid (<5 min) Cu(I)-catalyzed release of NO from GSNO (Fig. 1*b*), it is likely that copper-catalyzed reductive cleavage of GSNO also occurs *in vivo*.

The next question that arises is, of course, what is the source of reducing equivalents to regenerate Cu(I) following electron transfer to GSNO to release NO (Reaction 4)? Possible electron donors to Cu(II) are GSH (Reaction 5) and HbFe$^{II}$. With GSH as a donor, two molecules of NO would be released or two heme Fe$^{II}$NO adducts would be formed per molecule of GSSG produced. The mass spectrum reveals extensive formation of GSSG in the HbFe$^{II}$/GSNO incubates in the absence of chelators (Fig. 6*b*). Although a peak corresponding to its Na$^+$ adduct occurs at *m/z* 635, the expected GSSG peak at *m/z* 613 is not clearly evident in HbFe$^{II}$/GSNO incubates containing DTPA. Nonetheless, GSNO does release NO, as evidenced by the loss of GSNO peak intensity relative to the base peak at *m/z* 638 (Fig. 6, *c versus d*) and the formation of HbFe$^{II}$NO (Fig. 1*c* and Table II). Thus, reduction of [Cu(II)(DTPA)]$^{2-}$ by HbFe$^{II}$ was considered, which would account for the HbFe$^{III}$ absorbance seen in Fig. 2*a*. From Table II, 7.13 mM NO is released (6.97 mM HbFe$^{II}$NO and 0.16 mM HbFe$^{III}$NO) from the 15 mM GSNO present in the HbFe$^{II}$/GSNO/DTPA incubate. If all of the reducing equivalents were to come from GSH oxidation (Reaction 5), then 3.56 mM GSSG should be produced. However, HbFe$^{II}$ oxidation provides 1.44 milliequivalents of reductant (1.28 mM HbFe$^{III}$ and 0.16 mM HbFe$^{III}$NO), which would decrease the



SCHEME 1



SCHEME 2
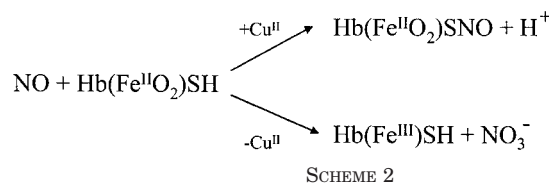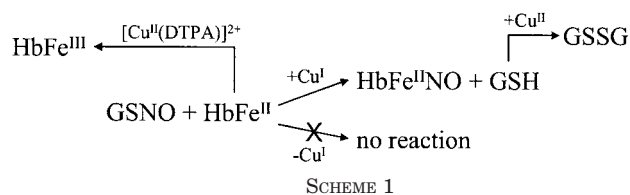
concentration of GSSG produced to 2.84 mM. This is approximately one-third of the GSSG produced in HbFe$^{II}$/GSNO incubates where a strong GSSG peak is observed at *m/z* 613. The lower than expected intensity of the GSSG (*m/z* 613) peak in Fig. 6*c* is attributed to ion suppression. The production of HbFe$^{III}$ in the HbFe$^{II}$ incubates in the presence but not the absence of DTPA (Table II) suggested that [Cu(II)(DTPA)]$^{2-}$ may accept an electron from HbFe$^{II}$, which was confirmed. The addition of authentic [Cu(II)(DTPA)]$^{2-}$ to HbFe$^{II}$ led to oxidation of 21% of the heme (Fig. 7). Electron transfer between [Fe(II)(EDTA)]$^{2-}$ and HbFe$^{III}$ has been reported previously (12).

No loss of $\nu$(SH) intensity was detected by FTIR when HbFe$^{II}$ was treated with GSNO with or without metal chelators (Fig. 4*a*). This is consistent with the proposal that the allosteric transition of Hb controls Cys$\beta^{93}$ *S*-nitrosation (33). The FTIR results also show that Cu(I) is required for HbFe$^{II}$NO formation because neocuproine inhibited blue shifting of the Cys$\beta^{93}$ $\nu$(SH) peak (Fig. 4*a*, *spectra 2* and *3*) that accompanies heme nitrosylation (29). The reactions in the HbFe$^{II}$/GSNO incubates reported here are shown in Scheme 1. Clearly the oxidation of HbFe$^{II}$ by [Cu(II)(DTPA)]$^{2+}$ is unlikely to be of importance *in vivo*, but the requirement of copper for NO release from GSNO shown in Scheme 1 could well have physiological relevance.

The key result that copper is also required for *S*-nitrosation of Cys$\beta^{93}$ of HbFe$^{II}$O$_2$ (4) can be deduced from Figs. 4*b* and 5*b*. *S*-Nitrosation of Cys$\beta^{93}$ is observed only in the absence of metal chelators (Fig. 4*b*, *spectrum 1*, and Fig. 5*b*). Thus, we propose Scheme 2 for the reactions of NO with HbFe$^{II}$O$_2$. NO is targeted to Cys$\beta^{93}$ in the absence of chelators, but in the presence of DTPA, all of the NO released from GSNO is targeted to the Fe$^{II}$O$_2$ heme (Figs. 3 and 4*b*) and converted to NO$_3^-$ (Reaction 6). Scheme 2 predicts that efficient Cu(II)–catalyzed *S*-nitrosation of Cys$\beta^{93}$ will preserve the biological activity of NO by preventing its conversion to nonvasoactive NO$_3^-$. The capture of NO by HbFe$^{II}$ (Scheme 1) should not lead to loss of its vasoactive power as long as Fe$^{II}$-NO adduct formation is reversible on a physiologically relevant time scale. It has been proposed that the Fe$^{II}$ heme centers of partially oxygenated Hb, as found in the RBC (1), have a much lower affinity for NO than fully deoxygenated HbFe$^{II}$ (9). Thus, copper control of NO reactivity with Hb, plus weaker binding of NO to HbFe$^{II}$ *in vivo* than *in vitro*, could explain why RBC Hb does not act a sink for most of the NO produced in the vascular system. A possible copper catalyst *in vivo* is copper-zinc superoxide dismutase, which is abundant in the RBC (34).

It is of interest to compare the extent of the prompt changes in HbFe$^{II}$ and HbFe$^{II}$O$_2$ on incubation with GSNO. When 15 mM GSNO is incubated with 15 mM (heme) HbFe$^{II}$ in the absence of metal chelators, 99% is converted to HbFe$^{II}$NO within 5 min, whereas only 46% of HbFe$^{II}$O$_2$ is converted to

HbFe$^{III}$ under the same conditions. This is easy to understand when we consider that ~7.5 mM NO released from GSNO was targeted to Cys$\beta^{93}$ in HbFe$^{II}$O$_2$ but not in HbFe$^{II}$ (Figs. 4 and 5). In the DTPA incubates 44% HbFe$^{II}$ *versus* 77% HbFe$^{II}$O$_2$ remain, and in neocuproine incubates 75% HbFe$^{II}$ *versus* 88% HbFe$^{II}$O$_2$ remain after the same 5-min period. Clearly, the increased stability of the Hb reactants in the presence of metal chelators is due to inhibition of GSNO breakdown, but the lower consumption of HbFe$^{II}$O$_2$ relative to HbFe$^{II}$ cannot be attributed to NO trapping by Cys$\beta^{93}$ in the former because this does not occur in the presence of chelators (Fig. 4*b*). More efficient NO trapping by HbFe$^{II}$ (35) than by HbFe$^{II}$O$_2$ ($k = 3$–$5 \times 10^7$ M$^{-1}$ s$^{-1}$ for Reaction 6) (36) would give rise to the higher HbFe$^{II}$ consumption in the incubates. Also, the reaction of NO with any free O$_2$ in the HbFe$^{II}$O$_2$ incubate would decrease the amount of HbFe$^{II}$O$_2$ consumed.

In this work we also examined the spectra of the HbFe$^{II}$/GSNO incubates after 1 h. The results obtained indicate that the prompt products undergo further reaction over longer times. For example, the Soret maximum after 1 h of HbFe$^{II}$/GSNO incubate still shows a maximum at 418 nm but with decreased intensity (data not shown). Because the spectrum of authentic HbFe$^{II}$NO in the absence of any glutathione-derived species is stable for >1 h, the HbFe$^{II}$NO initially formed must react with some reagent in the incubate.[2] The Soret maximum of the HbFe$^{II}$/GSNO/DTPA incubate after 1 h (data not shown) is blue-shifted (409 nm) from that at 5 min (411 nm) (Fig. 1*c*). We initially attributed this blue shift to increased HbFe$^{II}$NO formation caused by NO-driven reduction of HbFe$^{III}$ using reducing equivalents from GSH. However, the addition of GSH to authentic HbFe$^{III}$NO also gave rise to a Soret maximum at 411 nm and not the expected HbFe$^{II}$NO peak at 418 nm. The biological relevance of these slow reactions is questionable because, for example, any HbFe$^{III}$ formed in the RBC would be rapidly converted to HbFe$^{II}$ by methemoglobin reductase (37).

## CONCLUSIONS

The results reported here provide insight into the mechanism of heme nitrosylation following mixing of HbFe$^{II}$ with GSNO. The data presented are inconsistent with direct reduction of GSNO by HbFe$^{II}$ but are consistent with catalysis of GSNO breakdown by trace copper and *free* NO generation in the reactions. Because HbFe$^{II}$ is stable in the presence of GSNO when free copper is rigorously excluded from the system, direct reduction of GSNO by HbFe$^{II}$ is unlikely to be of biological significance. Trace copper also controls targeting of NO released from GSNO to the Cys$\beta^{93}$ and Fe$^{II}$O$_2$ centers of HbFe$^{II}$O$_2$. Thus, we conclude that copper catalysis of *S*-nitrosation and *S*-denitrosation plays a key role in preserving the vasoactivity of NO in the RBC.

## REFERENCES

1. Gross, S. S., and Lane, P. (1999) *Proc. Natl. Acad. Sci. U. S. A.* **96,** 9967–9969
2. Patel, R. P., Hogg, N., Spencer, N. Y., Kalyanaraman, B., Matalon, S., and Darley-Usmar, V. M. (1999) *J. Biol. Chem.* **274,** 15487–15492
3. Jia, L., Bonaventura, C., Bonaventura, J., and Stamler, J. S. (1996) *Nature* **380,** 221–226
4. Romeo, A. A., Filosa, A., Capobianco, J. A., and English, A. M. (2001) *J. Am. Chem. Soc.* **123,** 1782–1783
5. Singh, S. P., Wishnok, J. S., Keshive, M., Deen, W. M., and Tannenbaum, S. R. (1996) *Proc. Natl. Acad. Sci. U. S. A.* **93,** 14428–14433
6. Tsikas, D., Sandmann, J., Luessen, P., Savva, A., Rossa, S., Stichtenoth, D. O., and Frolich, J. C. (2001) *Biochim. Biophys. Acta* **1546,** 422–434
7. Pezacki, J. P., Ship, N. J., and Kluger, R. (2001) *J. Am. Chem. Soc.* **123,** 4615–4616
8. Pawloski, J. R., Hess, D. T., and Stamler, J. S. (2001) *Nature* **409,** 622–626
9. McMahon, T. J., and Stamler, J. S. (1999) *Methods Enzymol.* **301,** 99–114
10. Spencer, N. Y., Zeng, H., Patel, R. P., and Hogg, N. (2000) *J. Biol. Chem.* **275,** 36562–36567
11. Williams, D. L. H. (1999) *Acc. Chem. Res.* **32,** 869–876
12. Mauk, A. G., and Gray, H. B. (1979) *Biochem. Biophys. Res. Commun.* **86,** 206–210
13. Lei, Y., and Anson, F. C. (1995) *Inorg. Chem.* **34,** 1083–1089
14. James, B. R., and Williams, R. J. P. (1961) *J. Chem. Soc.* 2007–2019
15. Scorza, G., Pietraforte, D., and Minetti, M. (1997) *Free Radic. Biol. Med.* **22,** 633–642
16. Sheu, F. S., Zhu, W., and Fung, P. C. (2000) *Biophys. J.* **78,** 1216–1226
17. Antonini, E., Wyman, J., Brunori, M., Taylor, F. J., Rossi Farinelli, A., and Caputo, A. (1964) *J. Biol. Chem.* **239,** 907–912
18. Van Assendelft, O. W., and Zijlstra, W. G. (1975) *Anal. Biochem.* **69,** 43–48
19. Iorio, E. D. (1981) *Methods Enzymol.* **76,** 57–69
20. Antonini, E., and Brunori, M. (1971) *Hemoglobin and Myoglobin in Their Reactions with Ligands: Frontiers of Biology*, pp. 19–21, North-Holland Publishing Company, Amsterdam
21. Williams, W. J., Beantler, E., Erslev, A. J., and Rundles, R. W. (1972) *Hematology*, p. 11, McGraw-Hill Book Co., New York
22. Abbyad, P., Tromp, J., Lam, J., and Salin, E. (2001) *J. Anal. At. Spectrom.* **16,** 464–469
23. Dong, A. C., Huang, P., and Caughey, W. S. (1992) *Biochemistry* **31,** 182–189
24. Dong, A., Huang, P., and Caughey, W. S. (1990) *Biochemistry* **29,** 3303–3308
25. Mahalingam, T. R., Vijayalakshmi, S., Prabhu, R. K., Thiruvengadasami, A., Wilber, A., Mathews, C. K., and Shanmugasundaram, K. R. (1997) *Biol. Trace Elem. Res.* **57,** 223–238
26. Upmacis, R. K., Hajjar, D. P., Chait, B. T., and Mirza, U. A. (1997) *J. Am. Chem. Soc.* **119,** 10424–10429
27. Doyle, M. P., and Hoekstra, J. W. (1981) *J. Inorg. Biochem.* **14,** 351–358
28. Artz, J. D., and Thatcher, G. R. J. (1998) *Chem. Res. Toxicol.* **11,** 1394–1397
29. Sampath, V., Zhao, X. J., and Caughey, W. S. (1994) *Biochem. Biophys. Res. Commun.* **198,** 281–287
30. Dong, A., and Caughey, W. S. (1994) *Methods Enzymol.* **232,** 157–162
31. Kandori, K. (1998) *J. Am. Chem. Soc.* **120,** 5828–5829
32. Noble, D. R., and Williams, D. L. (2000) *Nitric Oxide* **4,** 392–398
33. Stamler, J. S., Jia, L., Eu, J. P., McMahon, T. J., Demchenko, I. T., Bonaventura, J., Gernert, K., and Piantadosi, C. A. (1997) *Science* **276,** 2034–2037
34. Gartner, A., and Weser, U. (1983) *FEBS Lett.* **155,** 15–18
35. Gow, A. J., Luchsinger, B. P., Pawloski, J. R., Singel, D. J., and Stamler, J. S. (1999) *Proc. Natl. Acad. Sci. U. S. A.* **96,** 9027–9032
36. Eich, R. F., Li, T., Lemon, D. D., Doherty, D. H., Curry, S. R., Aitken, J. F., Mathews, A. J., Johnson, K. A., Smith, R. D., Phillips, G. N., Jr., and Olson, J. S. (1996) *Biochemistry* **35,** 6976–6983
37. Kuma, F. (1981) *J. Biol. Chem.* **256,** 5518–5523

# Heme Nitrosylation of Deoxyhemoglobin by *S*-Nitrosoglutathione Requires Copper

Andrea A. Romeo, John A. Capobianco and Ann M. English

Access the most updated version of this article at doi: 10.1074/jbc.M202221200

Alerts:

- When this article is cited
- When a correction for this article is posted

Click here to choose from all of JBC's e-mail alerts

This article cites 34 references, 8 of which can be accessed free at
http://www.jbc.org/content/277/27/24135.full.html#ref-list-1